Cellular mechanisms of dendrite pruning in *Drosophila*: insights from in vivo time-lapse of remodeling dendritic arborizing sensory neurons

Darren W. Williams*,† and James W. Truman

Department of Biology, University of Washington, Seattle, WA 98195, USA
*Present address: MRC Centre for Developmental Neurobiology, King's College London, New Hunt's House, 4th Floor, Guy's Hospital Campus, London SE1 1UL, UK
†Author for correspondence (e-mail: dww@u.washington.edu)

Accepted 2 June 2005

Development 132, 3631-3642
Published by The Company of Biologists 2005
doi:10.1242/dev.01928

Summary

Regressive events that refine exuberant or inaccurate connections are critical in neuronal development. We used multi-photon, time-lapse imaging to examine how dendrites of *Drosophila* dendritic arborizing (da) sensory neurons are eliminated during early metamorphosis, and how intrinsic and extrinsic cellular mechanisms control this deconstruction. Removal of the larval dendritic arbor involves two mechanisms: local degeneration and branch retraction. In local degeneration, major branch severing events entail focal disruption of the microtubule cytoskeleton, followed by thinning of the disrupted region, severing and fragmentation. Retraction was observed at distal tips of branches and in proximal stumps after severing events. The pruning program of da neuron dendrites is steroid induced; cell-autonomous dominant-negative inhibition of steroid action blocks local degeneration, although retraction events still occur. Our data suggest that steroid-induced changes in the epidermis may contribute to dendritic retraction. Finally, we find that phagocytic blood cells not only engulf neuronal debris but also attack and sever intact branches that show signs of destabilization.

Key words: metamorphosis, pruning, local degeneration, EcR

Introduction

The nervous system is generated by progressive developmental phenomena, such as cell division and growth, and regressive phenomena, such as cell death and pruning (Cowan et al., 1984). One aspect of morphogenesis that is more pressing for neurons than other cell types is the elimination of extensive processes. Removal of such neuritic processes takes place in cells where the soma has undergone developmental cell death (Perry et al., 1983) and also in viable cells removing exuberant or inaccurate projections (Luo and O'Leary, 2005).

Selective branch removal, or pruning, is found throughout the vertebrate nervous system. Two of the best examples are the pruning of the sub-cortical axonal projections of Layer 5 neurons of the cortex (O'Leary and Koester, 1993) and the pruning of motoneurons at neuromuscular junctions (Keller-Peck et al., 2001). Both underscore the importance of this phenomenon in shaping neural circuitry, but represent two extremes of pruning. Layer 5 cortical neurons remove large identifiable lengths of axon from animal to animal; this has been termed 'stereotyped' pruning (Bagri et al., 2003). Pruning of motor axons in the vertebrate peripheral nervous system, by contrast, is usually small scale (i.e. local) and stochastic in nature.

The modes by which branches are eliminated also appear to vary. When motor axon branches lose their contacts, they lift off the muscle, form a 'retraction bulb' and retreat backwards to the parent branch (Keller-Peck et al., 2001). In contrast, chick retinal axons that 'overshoot' their targets within the optic tectum appear to correct errors by local degeneration of the axon (Nakamura and O'Leary, 1989). At present, we know little about the mechanisms that underlie either type of pruning, and how different they truly are.

Axonal and dendritic pruning is especially pronounced in insects that undergo complete metamorphosis. These insects build two distinct bodies: a larval form for feeding and growing, and an adult form for reproduction and dispersal. To transition between these two forms, the nervous system undergoes dramatic changes which include the differentiation of adult-specific neurons, the death of some larval neurons and remodeling of others (Levine and Weeks, 1996; Truman, 1996). Studies of central neurons in *Drosophila* have shown that pruning of axons and dendrites can be blocked by interfering with either ecdysone signaling (Schubiger et al., 1998; Schubiger et al., 2003; Lee et al., 2000), TGFβ signaling (Zheng et al., 2003) or the ubiquitin proteasome system (Watts et al., 2003). Alongside the requirement for such intrinsic factors, evidence is accumulating that extrinsic factors are also important for pruning in some neurons. Glial processes infiltrate the neuropil just prior to pruning of mushroom body γ neurons, and afterwards contain axonal debris (Watts et al., 2004). If glia are prevented from penetrating the neuropil, axon pruning is blocked (Awasaki and Ito, 2004).

The pruning of neuritic arbors is also seen in peripheral neurons in *Drosophila.* During metamorphosis, the majority of larval sensory neurons die but a small number persist to become functional adult neurons (Williams and Shepherd,

1999). Among those that survive are dendritic arborizing (da) sensory neurons (Usui-Ishihara et al., 2000; Williams and Shepherd, 2002). The large, complex dendritic arbors of these neurons are completely removed during early metamorphosis, before the cells elaborate their adult-specific arbors (Smith and Shepherd, 1996; Williams and Truman, 2004).

Here we describe how da neuron dendrites are deconstructed during early metamorphosis and the contributions of intrinsic and extrinsic factors to this process. We find that microtubule cytoskeleton remodeling precedes the severing of proximal dendrites, and that this intrinsic mechanism can be blocked by the expression of a dominant negative ecdysone receptor. Our data also suggest that two other cell populations may participate in the deconstruction of the arbor. Phagocytic blood cells attack and sever intact branches, and the epidermis, the substrate over which these cells arborize, remodels whilst the neurons are pruning.

Materials and methods

Fly stocks

For live imaging, *C161-GAL4* (Smith and Shepherd, 1996) and *ppk1.9-GAL4* drivers (Ainsley et al., 2003) were used to express either mCD8::GFP (Lee and Luo, 1999) or tubulin::GFP fusion proteins (Grieder et al., 2000) specifically in da neurons.

To disrupt ecdysone signaling, females of the genotype *UAS-EcR.B1-ΔC655.W650ATP1-9* (Cherbas et al., 2003) were crossed with *UAS-CD8::GFP*; *C161-GAL4, UAS-CD8::GFP/TM6b*. To block cell death, *UAS-p35* females were crossed to *UAS-CD8::GFP*; *C161-GAL4, UAS-CD8::GFP/TM6b*. To image the epidermis, we used a genomic rescue construct of histone H2A fused to GFP (Clarkson and Saint, 1999).

Staging of animals

Individual animals were collected at pupariation and maintained at 25°C. Staging was denoted as hours after puparium formation (h APF).

Immunocytochemistry and dye labeling

Dissection and immunohistochemistry were performed as described by Truman et al. (Truman et al., 2004). Primary antibodies included Rat anti-mCD8 (1:1000; Caltag Laboratories, Burlingame, CA, USA), mAb 22C10 [1:500; Developmental Studies Hybridoma Bank (DSHB), Iowa City, IA, USA] and anti-Cut (F2) (1:20, DSHB). Secondary antibodies included; 488 Alexa Fluor anti-rabbit IgG (1:500; Molecular Probes, Eugene, OR, USA) and Texas Red donkey anti-mouse IgG (1:500; Jackson ImmunoResearch Laboratories, West Grove, PA, USA).

Acidic organelles were labeled with LysoTracker Red (Molecular Probes). A 1 nl bolus of 50% LysoTracker DND-99 was injected directly into prepupa 10 h APF using a pico-spritzer and a glass microneedle.

Image acquisition and processing

Confocal images were taken using a BioRad (Hercules, CA, USA) Radiance 2000 system equipped with a krypton–argon laser. Z-stacks were collected at 1.5 μm intervals (40×). For time-lapse imaging, individual prepupae or pupae were mounted in an imaging chamber (Williams and Truman, 2004) and data acquired with the same Radiance system using a Ti:Sapphire laser (Spectra-Physics, Fremont, CA, USA) set at 905 nm. Time-lapse frames consisted of stacks of ~25 sections at 1.5 μm intervals, acquired every 10 minutes. Stacks and movies were assembled in ImageJ, adjusted for brightness and contrast using Photoshop (Adobe Systems, San Jose, CA, USA).

Results

Dorsal dendritic arborizing (da) sensory neurons of the abdomen

The dorsal neurons labeled by *C161-GAL4* were individually identified by dendritic morphology and levels of Cut protein expressed (Grueber et al., 2002; Grueber et al., 2003) (Fig. 1A). Two da neurons, ddaD and ddaE, have simple dendritic arbors and show no measurable Cut expression. The dendritic arbor of ddaD projects anteriorly whereas that of ddaE projects posteriorly. Two other da neurons show high levels of Cut protein and have spike-like protrusions on their branches, identifying them as ddaF and ddaA. A fifth da neuron, ddaB, has low levels of Cut and a simpler arbor. A sixth neuron expresses GFP at low levels. Using transgenes containing regulatory regions from the gene *pickpocket* (*ppk*), we identified it as ddaC.

Deconstruction of the larval da sensory system

The five dorsal da neurons strongly labeled by *C161-GAL4* show two different fates: ddaA, ddaB and ddaF undergo cell death, whereas ddaD and ddaE survive and remodel. Neither group shows any obvious change at 0 h APF (data not shown). By 6 h APF the arbors of ddaF, ddaB and ddaA have largely disappeared, although some fragments and blebs of GFP remain (Fig. 1B). The corpses of the cell bodies of these neurons can be seen in close proximity to the nerve.

The dendrites of ddaD and ddaE are still larval in their number and extent at 6 h APF. By 10 h APF (Fig. 1C), they have started to prune, with arbor loss more advanced in ddaE than ddaD. Filopodia are also found on the branches of both neurons. By 16 h APF, many of the higher order branches are lost, and detached branches appear to be separated from the main arbor (Fig. 1D). Filopodia are still found along the branches as the proximal regions begin to thin. By 24 h APF, the only remaining dorsal neurons that express the *C161-GAL4* driver are ddaD, ddaE and dbd. Debris derived from pruned dendrites remain, and the cell bodies have filopodia-rich growth cones (Fig. 1E). Axons remain intact throughout and show no change in caliber.

The cellular dynamics of death

To understand the cellular mechanisms that bring about these dramatic changes, we used in vivo time-lapse microscopy. Fig. 2A shows frames from Movie 1 (see supplementary material) focusing on the distal arbors of 3 da neurons. The neurons imaged are ddaF and ddaB, both of which die, and ddaD, which survives and remodels.

At 0 h APF, the dendritic arbors are indistinguishable from their larval form. By 2 h APF, the dorsally projecting branch of ddaF develops constrictions and swellings which become more obvious ‘beads’ by 3 h APF. Between 3 and 4 h APF, the branch severs at multiple sites, leaving blebs of GFP, which move away randomly. The other branches of ddaF follow the same sequence.

Between 3 and 4 h APF, the dendrites of ddaB also begin to generate constrictions and beads. Just after 5 h APF its branches sever, leaving only the arbor of ddaD intact by 6 h. The dying cells showed no filopodia. Beading appears to propagate through the arbor as a proximal to distal wave. Fig. 2B illustrates this wave in the dorsally projecting arbor of ddaF.

At 1.5 h a distinct bead forms in the proximal region whereas the most distal part is intact. By 3 h the whole branch appears beaded, and by 4 h these beads move in random directions.

To visualize the microtubule cytoskeleton in these neurons, we used a tubulin GFP fusion protein, tub::GFP. At 0 h APF, the arbors have a uniform distribution of tub::GFP (data not shown). By 3 h APF, ddaF shows a redistribution of tub::GFP (Fig. 2C), with some regions losing tub::GFP while others accumulate it into beads. In contrast, the arbor of ddaD at 3 h APF still shows a uniform distribution of tub::GFP.

When p35 was expressed with *C161-GAL4*, cell death was blocked in ddaA, ddaF and ddaB (Fig. 2D). The distal dendrites of ddaF and ddaB did not bead and undergo degeneration by 5 h APF (Fig. 2D). At 18 h APF the cell bodies of these 'rescued' da neurons were still evident, but their arbors had been largely removed (Fig. 2E) and abundant filopodia extend from all cells.

The cellular dynamics of pruning

To obtain a greater understanding of dendritic pruning in remodeling neurons, we made time-lapse movies of ddaD and ddaE. Fig. 3A shows selected frames from a movie between 14 and 24 h APF (Movie 2 in supplementary material). At 14 h 10 min APF <50% of the arbors of ddaD and ddaE remain, with filopodia found throughout. Severed branches, along with smaller fragments and blebs of GFP are seen close by. By 17 h 10 min APF more branches are severed. The primary branch of ddaE is also thinner than at 14 h 10 min APF. By 19 h APF the major branches of both neurons have been severed from their cell bodies. Between 19 and 24 h APF the separated branches decrease in length, thin and form swellings.

Movies of ddaD and ddaE taken during this period (n=8) reveal that branch severing occurs at both distal and proximal sites within the arbor. Fig. 3B shows selected frames from Movie 2 (in supplementary material), focusing on the proximal arbor. Large and small swellings are found along the primary branches of both ddaD and ddaE throughout the thinning phase and move in both proximal and distal directions. Another feature coincident with the thinning is the appearance of filopodia, which extend and retract in the thinning zone (17 h 00 min). Between 17 h 00 min and 17 h 50 min the caliber of the primary branch of ddaE becomes noticeably thinner and changes from straight to undulating. Just prior to 18 h the primary branch of ddaE is severed. The primary branch of ddaD continues to thin and severs at 18 h 30 min.

Fig. 3C shows a ddaD branch undergoing a 'distal' severing event. At 14 h 10 min the arbor appears stable, although there are swellings similar to those described above for proximal severing. Between 15 h 10 min and 15 h 20 min the branch severs, but shows no obvious thinning prior to this event.

Severed branches undergo fragmentation as illustrated in Fig. 3D. At 17 h 50 min the segment begins to thin and generate swellings. At 18 h 50 min the branch is beaded and is fragmenting into blebs. By 20 h most debris has disappeared.

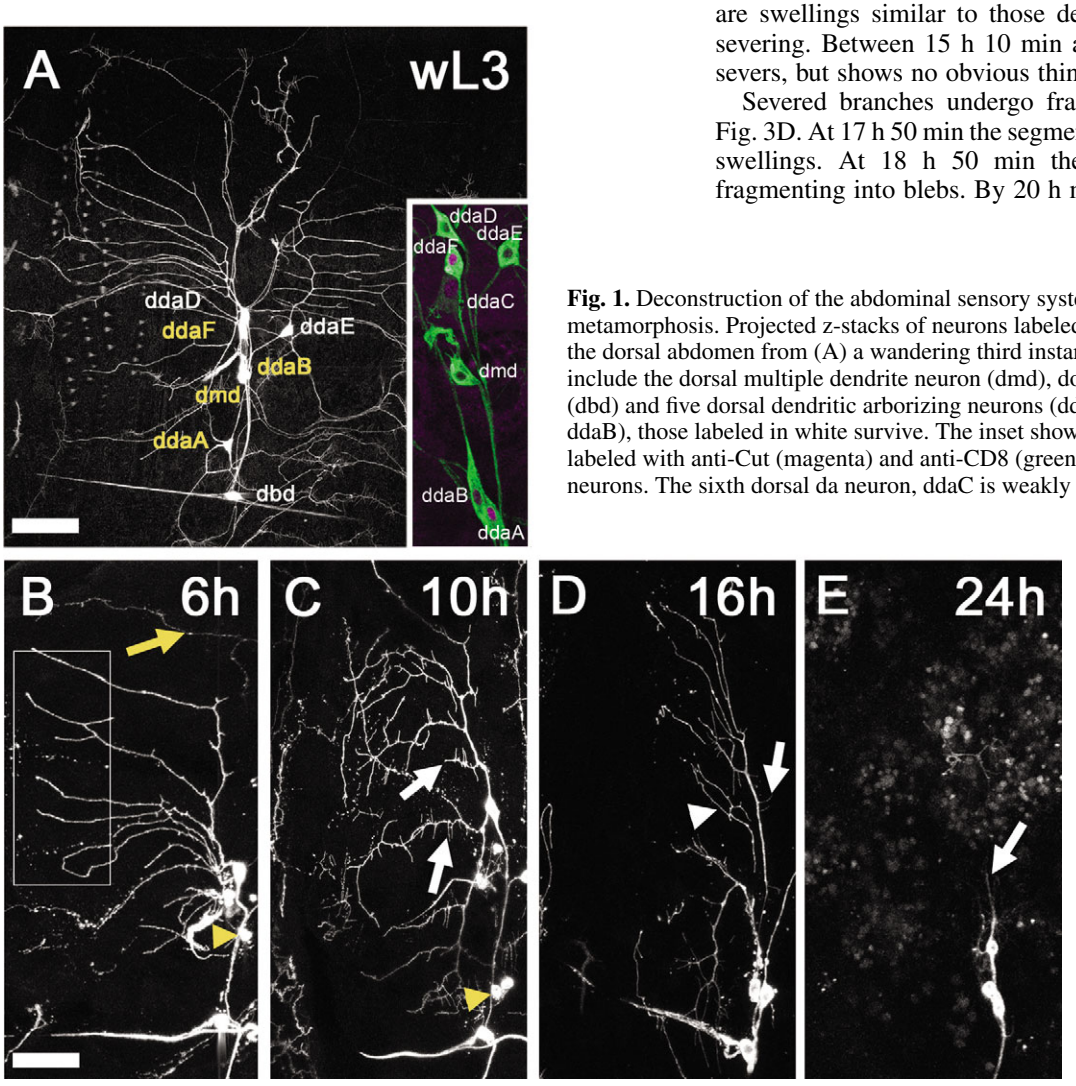

Fig. 1. Deconstruction of the abdominal sensory system during early metamorphosis. Projected z-stacks of neurons labeled by *C161-GAL4>CD8::GFP* in the dorsal abdomen from (A) a wandering third instar larva (wL3). Neurons labeled include the dorsal multiple dendrite neuron (dmd), dorsal bipolar dendrite neuron (dbd) and five dorsal dendritic arborizing neurons (ddaD, ddaE, ddaF, ddaA and ddaB), those labeled in white survive. The inset shows merged projected z-stacks labeled with anti-Cut (magenta) and anti-CD8 (green) to allow identification of neurons. The sixth dorsal da neuron, ddaC is weakly labeled. Scale bar: 90 μm. (B) By 6 h APF the arbors of ddaF, ddaB and ddaA have largely disappeared (yellow arrow). The cell bodies of dead cells are found close to the nerve (yellow arrowhead). The dendrites of ddaD are still intact. Box denotes region imaged in Fig. 2A. Scale bar: 40 μm. (C) At 10 h APF ddaD shows signs of pruning. (D) At 16 h APF the higher order branches are gone and detached branches are found near the arbor (arrowhead). The proximal branch is thinning. (E) At 24 h APF only ddaD, ddaE and dbd remain. Note filopodia on pruning branches (white arrows). Dorsal is up and anterior to the left.

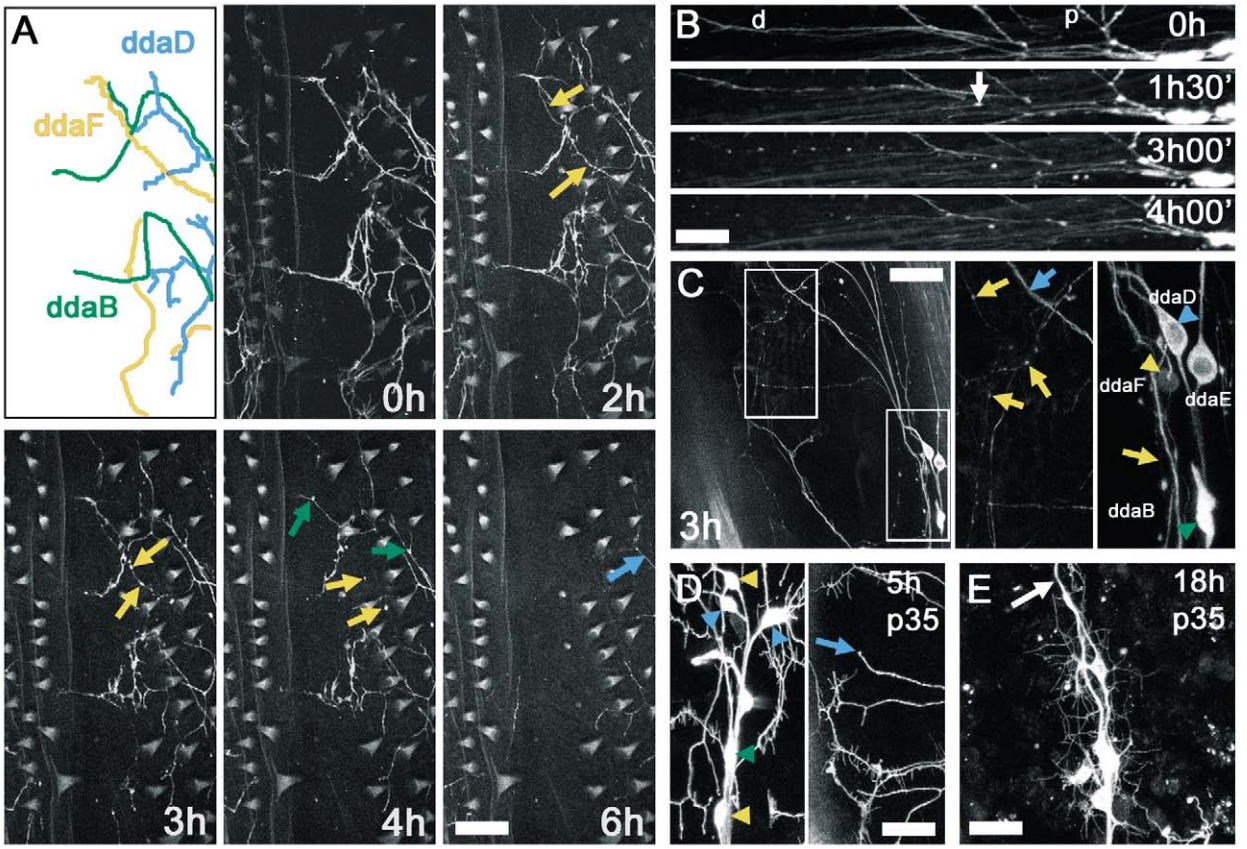

Fig. 2. Dynamics of dying da neuron dendrites. (A) Frames from Movie 1 (see supplementary material) of wild-type neurons (*C161-GAL4>CD8::GFP*) in the dorsal region of the prepupa (boxed region in Fig. 1B). The drawing shows distal arbors of ddaF (yellow), ddaB (green) and ddaD (blue) at 0 h APF. At 0 h arbors have a uniform caliber indistinguishable from those of the larva. By 2 h APF the dorsal branch of ddaF develops constrictions and swellings (yellow arrows). By 3 h APF the swellings become bead-like (yellow arrows). Between 3 and 4 h APF the branch severs, leaving blebs of GFP. The branches of ddaB generate swellings (green arrows). Between 4 and 6 h they sever, and the GFP blebs rapidly disappear, leaving only ddaD intact (blue arrow). Scale bar: 20 μm. (B) Projected z-stacks of ddaF in a wild-type animal (*C161-GAL4>CD8::GFP*). Cell bodies and proximal arbor (p) are shown on the left with the distal (d) dorsally projecting arbors on the right. At 1 h 30 min a distinct bead forms at a proximal branch point (arrow), whereas the most distal part (to the right) is intact. By 3 h the distal region is completely beaded. At 4 h the beads have moved position. Scale bar: 25 μm. (C) Projected z-stack of dorsal abdomen of wild-type (*C161-GAL4>tub::GFP*) at 3 h APF. The distal and proximal regions (boxed) are shown in the panels on the right. The distal arbor of ddaF has distinct beads (yellow arrows) whereas ddaD has a uniform distribution of *tub::GFP* (blue arrow). The nucleus and the proximal branches of ddaD and ddaE are intact, next to remains of ddaF (yellow arrowhead) and ddaB (green arrowhead). Dorsal is up and anterior to the left. Scale bar: 40 μm. (D) p35 inhibits cell death in all neurons expressing GFP and p35 at 5 h APF (*C161-GAL4>CD8::GFP, p35*). Left panel shows intact cell bodies; arrowheads indicate ddaF and ddaA (yellow), ddaB, (green), and ddaD and ddaE (blue). The arbor of ddaD (blue arrow) would normally be the only one left by this time in development. Right panel shows distal arbors of the same cells. Scale bar: 30 μm. (E) At 18 h APF all neurons are still alive in *C161-GAL4* animals expressing p35. Arrow indicates intact primary branches of ddaB and ddaF. Scale bar: 30 μm.

In addition to severing and fragmentation, the branches of ddaD and ddaE can also undergo distal to proximal retraction. Fig. 3E shows a movie sequence in which retraction occurs in the proximal region of ddaD. At 16 h 30 min the primary branch of ddaD possesses a number of filopodia. Between 16 h 30 min and 20 h 00 min the branch retreats retrogradely towards the cell body. We saw retraction events in the distal regions of the arbor (branch labeled with asterisk in Fig. 3C retracts after severing event). While branches are retracting distally they may be severed at more proximal sites. Interestingly, severed branches can retract at both ends before undergoing fragmentation.

Dendrite thinning and cytoskeletal dynamics

Because branch thinning precedes proximal severing, we examined the cytoskeleton in this region (Fig. 4A) during pruning using 22C10, a monoclonal antibody against the microtubule-associated protein Futsch (Hummel et al., 2000). The proximal branches of ddaC in third instar larvae have a uniform caliber (Fig. 4B) and even staining with 22C10 (Fig. 4B′). Following the onset of metamorphosis, the proximal branches thin and generate swellings (Fig. 4C). Futsch is redistributed showing clear gaps in staining where branches are constricted, and high levels in the beads (Fig. 4C′). The emergence of filopodia on these branches indicates that the actin cytoskeleton is also being locally remodeled.

To examine the dynamics of the microtubule cytoskeleton, we made time-lapse movies of tub::GFP in ddaC (Movie 3 in supplementary material; Fig. 4D). At 0 h APF proximal arbors show uniform distribution of tub::GFP. By 2 h APF tubulin is

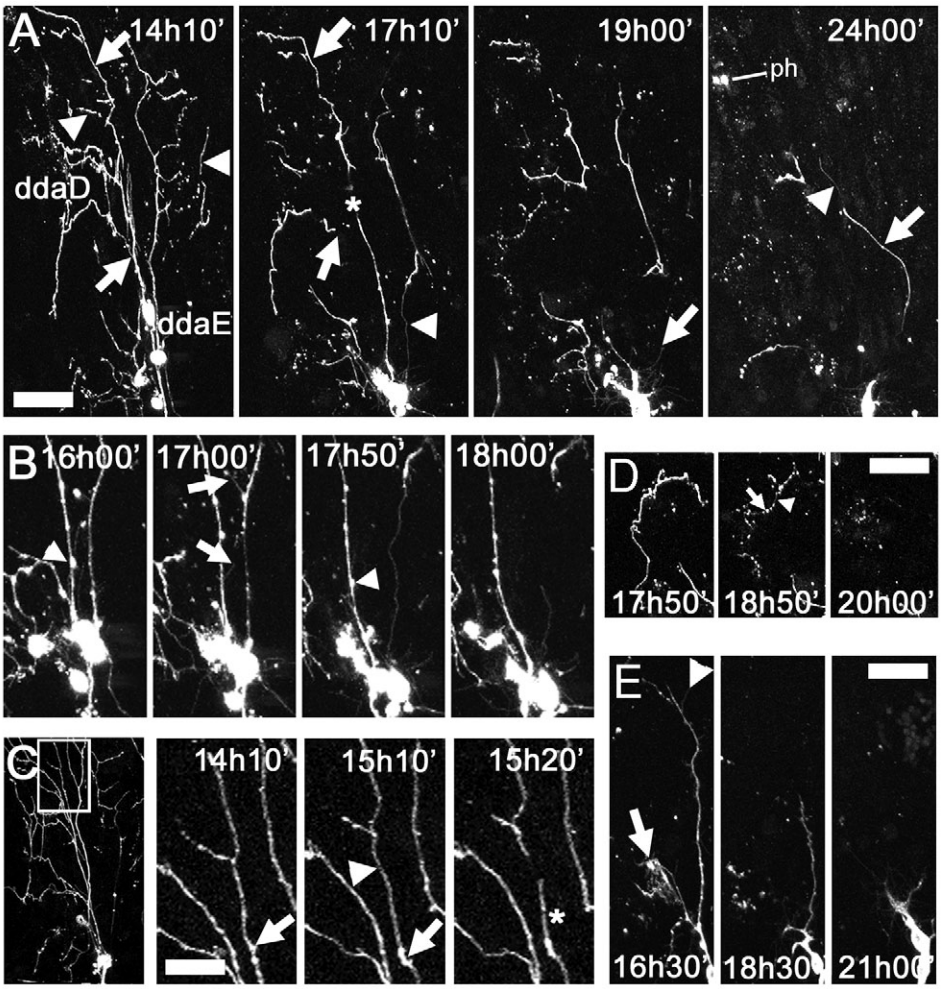

Fig. 3. The dynamics of dendritic pruning. Projections of z-stacks taken from movies of a wild-type pupae (*C161-GAL4>CD8::GFP*). (A) Overview of Movie 2 (see supplementary material). At 14 h 10 min APF as the arbors of ddaD and ddaE are pruning, fragments and blebs of GFP are found close to the arbor (arrowheads). Filopodia extend on ddaD's primary branch (arrows indicate sites of future severing). By 17 h 10 min ddaD has severed at two sites (arrows). The primary branch of ddaE is thinned (arrowhead). Asterisk indicates where arbor temporarily moved out of the z-stack. By 19 h 00 min the primary branches of both neurons have been separated from the cell body. Filopodia extend from the cell bodies (arrow). Between 19-24 h the severed branches decrease in length, thin (arrowhead) and generate swellings (arrow). Scale bar: 40 μm. (B) Proximal thinning of dendrites. Selected frames from Movie 2 focusing on a proximal region of ddaD and ddaE. Arrowheads indicate beads. Filopodia extend and retract on the thinning branch throughout the sequence (arrows, 17 h 00 min). Between 17 h 00 min and 17 h 50 min ddaE's primary branch becomes noticeably thinner. Just prior to 18 h ddaE is severed, isolating the distal arbor. (C) Distal branch severing. Overview of distal severing in ddaD; box indicates area enlarged in the panels on the right. At 14 h 10 min beads are present at the site labeled with the arrow. The beads are dynamic and change position during the movie. At 15 h 10 min there is no obvious thinning at the site where the arbor will sever (arrowhead) Branch labeled with asterisk retracts a short distance following severing. Scale bar: 20 μm. (D) Branch fragmentation. Branch severed from the primary branch (lower arrow in A) shows thinning at the ends by 17 h 50 min. At 18 h 50 min the branch begins to fragment into blebs, and by 20 h 00 min the only trace of the branch are a few blebs of GFP remaining in the field. Arrow indicates beads; arrowhead denotes thinning. Scale bar: 40 μm. (E) Branch retraction. Frames from a movie showing a retraction event on the primary branches of ddaD. The primary branch shows dynamic filopodia (arrowhead) along its length. Retraction is evident at 18 h 30 min and is back to it cell body by 21 h 00 min. The ventral branch to the left undergoes fragmentation (arrow). Scale bar: 35 μm.

redistributed and non-uniform. By 4 h APF, there is significant loss of tub::GFP in some regions while it is aggregated in large beads in other regions. These data show that a local loss of the microtubule cytoskeleton is associated with regions that undergo dendritic thinning.

Hormonal control of da neuron pruning

The pruning of da neuron dendrites occurs in the broader context of the dismantling of a larval body through the actions of the steroid hormone ecdysone and its metabolites. To establish the relative contributions of cell-autonomous versus non cell-autonomous mechanisms, we blocked ecdysone signaling in the neurons using a dominant negative version of the ecdysone receptor (EcR^{DN}).

When EcR^{DN} is expressed in ddaA, ddaF and ddaB, cell death is blocked and the dendrites of these cells remain intact (Fig. 5B). Similarly ddaD and ddaE fail to prune properly; no severed branches or cellular debris are evident, and the proximal arbor does not 'thin' (Fig. 5B). Instead the distal tips of the dendritic arbors of these neurons show bulb-like swellings, similar to retraction bulbs (Fig. 5E,F).

Time-lapse movies of EcR^{DN}-expressing ddaD and ddaE (Movie 4 in supplementary material) reveal how branches are removed (Fig. 5G). At 16 h APF the arbor shows features described above with prominent retraction bulbs forming on the distal tips of dendrites. By 24 h 10 min APF the branches have shortened and the retraction bulbs have increased in size. The subsequent frames show a slow but steady progression of retraction towards the cell body. One branch in ddaE (Fig. 5G, 25 h 30 min) was seen to sever during retraction. This was the only severing event seen in five movies and it was not preceded by thinning. Thinning was never seen in the proximal region of the dendritic arbor, and even at 64 h APF EcR^{DN}-expressing neurons still possess vestiges of larval branches and show no sign of adult outgrowth (data not shown).

Although the expression of EcR^{DN} suppressed branch

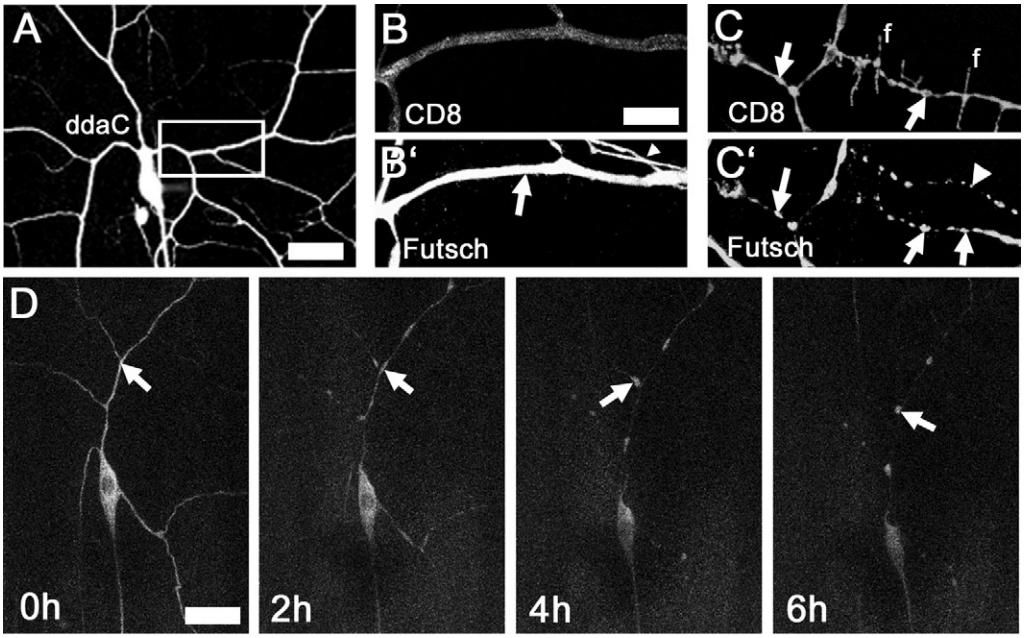

Fig. 4. Cytoskeletal remodeling of dendrites during early metamorphosis. (A) Projected confocal z-stack of ddaC in the abdomen of a wild-type larva (*ppk1.9GAL4> CD8::GFP*). The box denotes the region from which images B-C′ were collected. Scale bar: 30 μm. (B,B′) The proximal branch of ddaC at wandering third instar larva stage labeled with anti-CD8 (B) and anti-Futsch (B′). Arrowhead indicates branches from another da neuron. (C,C′) The proximal branch of ddaC at 3 h APF labeled with anti-CD8 (C), anti-Futsch (C′); arrows denote beads on branches. Filopodia (f) are found on branches that have undergone thinning; arrowhead indicates another da neuron. Scale bar: 10 μm. (D) Dynamics of the microtubule cytoskeleton of ddaC during the first six hours of metamorphosis. Projections of z-stacks from a movie showing tub::GFP distribution. 0 h APF reveals the uniform distribution of tub::GFP. By 2 h APF tubulin is redistributed resulting in a decrease in some places and an increase (arrow) in others. By 4 h APF some regions lose significant quantities of tub::GFP while others accumulate it into beads (arrow). By 6 h APF very large beads have formed that are separated by lengths of arbor that have little to no GFP signal. Scale bar: 30 μm.

severing and local degeneration, the branches show a retrograde retraction. This retraction may be due either to an ecdysone-induced cellular program that is not blocked by EcR^{DN} or to the neurons' response to changes in the epidermis, i.e. the substrate on which they arborize. Consequently, we examined the changes taking place in the epidermis during early metamorphosis.

Metamorphic remodeling of the abdominal epidermis

The dendrites of ddaD and ddaE arborize over a discrete region of the dorsal larval epidermis. In the early pupa the abdominal epidermis consists of two populations of cells, large polyploid larval cells and small diploid cells of the imaginal histoblast nests (Fig. 6A). To visualize how the epidermal target remodels relative to the pruning neuron, we used a histone GFP fusion line. Movie 5 (in supplementary material) shows the cells of the dorsal histoblast nests beginning to spread dorsally. Fig. 6 shows how a larval epidermal cell is consumed by phagocytic blood cells. At 15 h 00 min the large nucleus of the larval cell is intact and the diploid nuclei of phagocytic blood cells are close by. By 17 h 20 min the cell has been consumed by the phagocyte. The remnants of the larval cell (i.e. nuclear GFP) are within the phagocyte and allow it to be tracked. Fig. 6C summarizes the fate of 106 larval epidermal cells imaged in Movie 5. The 17 cells (i.e. 16% of population) labeled with orange dots die by 25 h APF and 70% of those cells are found distant from the histoblast migration front. Movie 5 also shows that after a larval cell is removed, the epidermis reorganizes to compensate for the gap. Hence, during the time that the da neurons are pruning back their dendrites, the underlying epidermis is in a state of flux as larval cells are being removed throughout the domain of innervation. This removal of larval cells may play a role in directing the behavior of distal dendrites during this period.

The role of phagocytes in dendritic pruning

Besides their role in removing dead and dying cells during metamorphosis, blood cells appear to be intimately involved in pruning dendrites. Migratory cells labeled with GFP were found in most of the pupae with GFP-expressing da neurons ('ph' in Fig. 3A; 24 h 00 min and Movie 2). Fig. 7A shows a faintly labeled phagocyte entering the field from the top right. By 19 h 40 min a severed branch from ddaE shows beading and the phagocyte moving into close proximity. At 19 h 50 min the branch fragments, and by 22 h 00 min has disappeared and the GFP has been transferred to the phagocyte through engulfment of labeled dendrite fragments. In Fig. 7B such a phagocyte is co-labeled with the acidotropic marker LysoTracker. These cells are not glia, since they did not label with repo-GAL4 but instead express hemolectin-GAL4, a phagocytic blood marker (data not shown).

Phagocytes also appear to play an active role in severing intact dendritic branches. Such attacks can occur at the distal tips of branches or at proximal sites near the cell body. Fig. 7C shows selected frames from a time-lapse sequence where the distal part of the primary branch of ddaE is being attacked by phagocytes. At 16 h 00 min a phagocyte enters the field from the top right and comes into contact with the distal tip of ddaE. By 17 h 00 min the distal part of the branch is gone and the phagocyte appears to be labeled with more CD8::GFP. At 17 h 00 min another phagocyte moves from the left field. This phagocyte attacks the end of the primary branch as it retracts.

Phagocytes can also attack proximal regions of the dendritic arbor. Fig. 7D shows a time-lapse sequence (movie 6) from 15 h 40 min APF focusing on interactions between a phagocyte

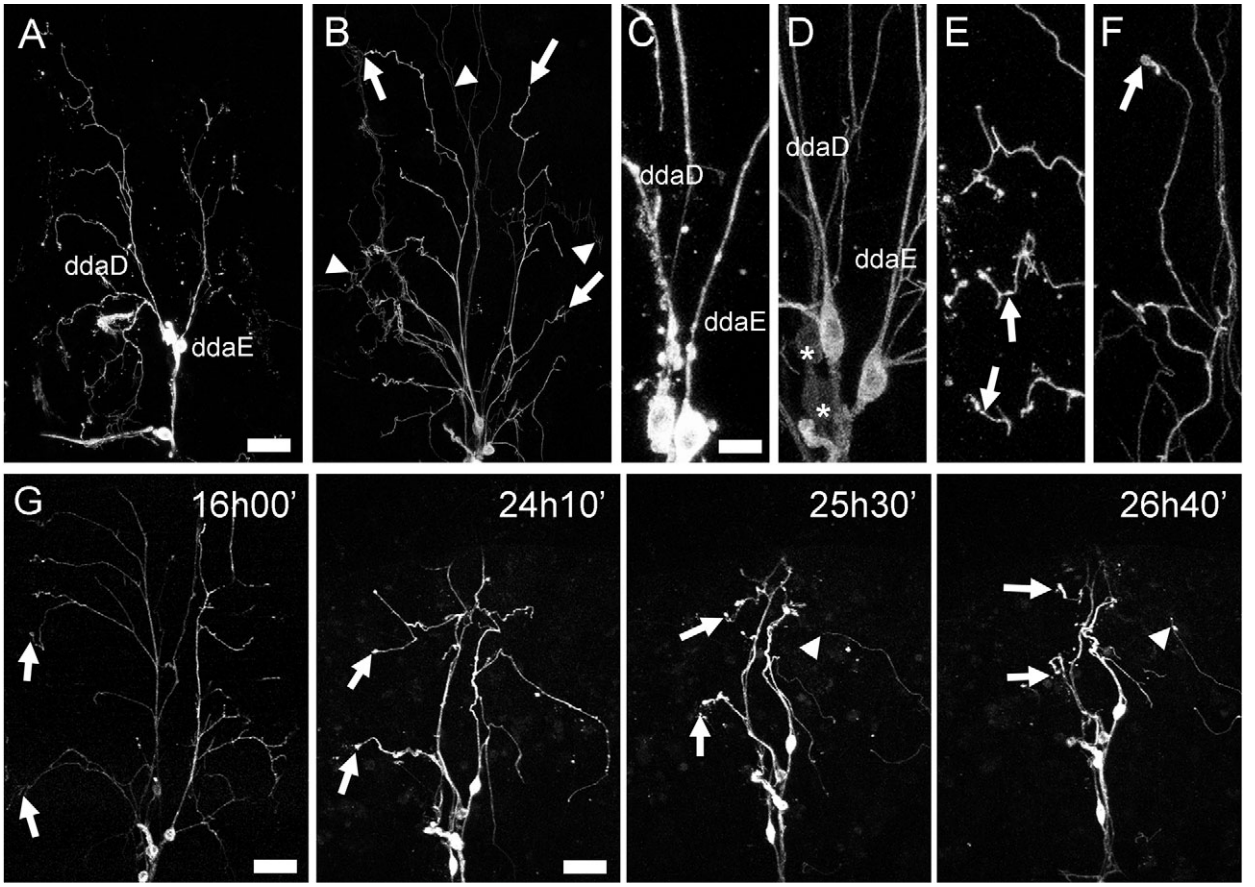

Fig. 5. Blocking ecdysone signaling in da neurons with EcR^{DN}. (A) Projected z-stack of wild-type neurons (*C161-GAL4>CD8::GFP*) in the dorsal abdomen at 16 h APF. (B) Projected z-stack of neurons expressing EcR^{DN} (*C161-GAL4>EcR^{DN}; CD8::GFP*) in the dorsal abdomen at 16 h APF. No severed branches are present and only a few blebs of GFP are evident. Arrows indicate distal dendrites of ddaD and ddaE, arrowheads the distal dendrites of ddaF. Scale bar: 20 μm. (C) The proximal branches of dorsal da neurons in a wild-type animal at 16 h APF are thinned. Scale bar: 7 μm. (D) Equivalent proximal branches of dorsal da neurons expressing EcR^{DN} at 16 h APF show no thinning. Asterisk indicates cell bodies of ddaF and ddaB still present. (E) Distal region of branch in a wild-type animal at 16 h APF. Arrows indicate fragments. (F) Distal region of ddaD expressing *EcR^{DN}* at 16 h APF. Arrow indicates retraction bulb. (G) Dynamics of the pruning of dorsal da neurons expressing EcR^{DN} during early metamorphosis. Arrows indicate branch retraction. At 24 h APF the dendrite branches are shorter and the retraction bulbs have increased in size. Branches continue to retract (arrows). Arrowhead in 25 h 30 min and 26 h 40 min identifies a distal severing event. Scale bar: 20 μm (16 h APF); 25 μm (other times).

and the proximal region of ddaE. Between 15 h 40 min and 17 h 30 min the phagocyte moves close to the pruning arbor. Between 18 h 10 min and 18 h 20 min the branch is severed where the phagocyte is located. A small bleb of GFP derived from the pruning branch appears to be internalized by the phagocyte at severing (18 h 30 min).

We found the behavior of phagocytes to differ if they encountered neurons expressing EcR^{DN}. Fig. 8A shows a typical phagocyte from a wild-type animal (*C161-GAL4>CD8::GFP*). The path of the phagocyte shows it tracking around a proximal branch of ddaD, which is undergoing fragmentation, then after severing the primary branch it moves to the right and attacks the retracting branch of ddaE. In contrast a phagocyte found near the proximal arbor of neurons expressing EcR^{DN} (Fig. 8B) moves slowly across the field, showing little pseudopod activity, and fails to attack the proximal arbor. The phagocyte on the left in Fig. 8B follows a retracting distal tip, through the 8h 20 min of the movie, and removes pieces of the retraction bulb as the branch retracts (also see Movie 4 in supplementary material).

Discussion

The abdominal sensory system of the adult fly is a mosaic consisting of postembryonic neurons derived from the imaginal histoblast nests and genital disk (Hartenstein and Posakony, 1989; Taylor, 1989), and a subset of larval sensory neurons of embryonic origin (Williams and Shepherd, 1999; Williams and Truman, 2004). At the onset of metamorphosis, larval sensory neurons either die or survive and remodel. Among the dorsal neurons of abdominal segments 2-5, we found that ddaA, ddaF and ddaB die whilst ddaC, ddaD and ddaE survive.

The dendritic arbors of neurons that die undergo local degeneration

Programmed cell death is a near ubiquitous phenomenon in the vertebrate nervous system and essential for proper morphogenesis (Burek and Oppenheim, 1996), Surprisingly, most studies have focused on the cell body and paid little attention to the fate of neuritic processes, even though the

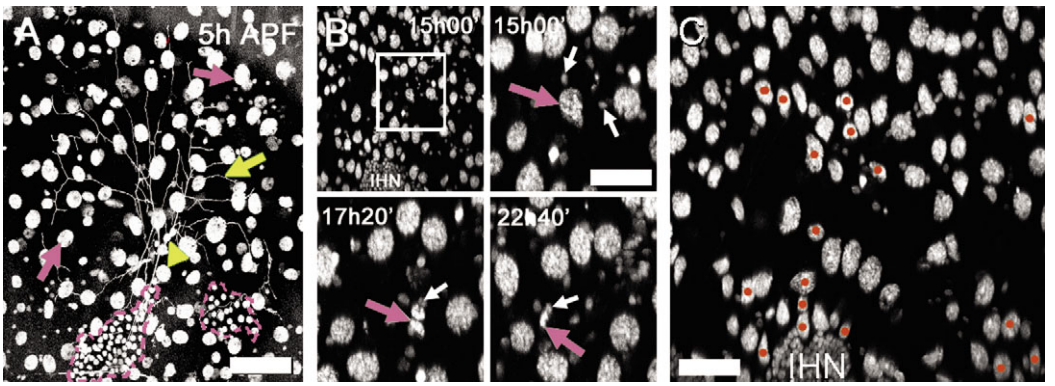

Fig. 6. Remodeling of the abdominal epidermis. (A) The position of ddaD and ddaE (yellow arrow/arrowhead) in relation to the larval epidermal cells (pink arrows) and smaller diploid cells of the histoblast nests (pink outline) at 5 h APF in a *H2Av::GFP, C161-GAL4>CD8::GFP* animal. Scale bar: 45 μm. (B) Removal of larval epidermal cells by phagocytes. Projections of z-stacks from a movie with *H2Av::GFP* labeling the nuclei of all cells. The boxed region shows the position of the other enlarged images relative to the imaginal histoblast nest (IHN). At 15 h 00 min the larval epidermal cell nucleus is intact (pink arrow), and the small diploid nuclei of phagocytic blood cells (white arrows) are found close by. Between 16 h 40 min and 17 h 20 min the nucleus moves and changes shape, identifying that it has been consumed by a phagocyte. For the remainder of the movie the remnants of the nucleus can be seen inside the phagocyte. Scale bar: 35 μm. (C) Fate of 106 larval epidermal cells during early metamorphosis (14 and 25 h APF). During this time period, 17 larval epidermal cells died (orange dots). Scale bar: 50 μm.

axons of most projection neurons have reached their targets before the onset of cell death (Perry et al., 1983).

We used time-lapse imaging to observe the dendrites of dying neurons in intact animals. The distal branches of the ddaF develop swellings at 2 h APF that become distinct beads, which accumulate tubulin. Between 3 and 4 h APF branches undergo severing at multiple sites where they have thinned. This beading propagates through the arbor in a proximal to distal direction with proximal changes occurring 20-30 minutes ahead of the distal ones (Fig. 2C). This same progression is seen in ddaB but with a lag of 1 hour. A similar degeneration is found in the peripheral arbors of Rohon-Beard neurons, which also thin and fragment when dying (Reyes et al., 2004).

The destruction of peripheral processes has been most widely studied following acute local trauma, where the axon branch distal to the lesion undergoes a stereotyped degeneration by fragmentation, termed Wallerian degeneration (Waller, 1850; Beirowski et al., 2005). There are similarities between the degeneration of dendrites in our study and the axon pathology seen in Wallerian degeneration. Firstly, in vitro models of Wallerian degeneration reveal a proximal to distal spread of beading in the separated distal neurites (Sievers et al., 2003). Secondly, the microtubule cytoskeleton is disrupted following transection (Zhai et al., 2003) and the beaded morphology and redistribution of tubulin we see in the da neuron dendrites resembles that seen in neurons treated with microtubule depolymerizing drugs (He et al., 2003).

We found that the expression of EcR^{DN} in neurons that were fated to die blocked their death and prevented the local degeneration seen between 3 and 6 h APF (data not shown). This prompted us to ask whether the degeneration normally observed is due to cell death directly or is the result of a hormone-induced microtubule disassembly program running in parallel with cell death. When we block cell death by expressing p35, the dendrites showed no signs of degeneration by 5 h APF (Fig. 2D), yet by 18 h APF their arbor was largely removed (Fig. 2E). Thus, with p35, the dendrites of these doomed cells prune at the same time and in the same way as ddaD and ddaE (data not shown), suggesting that under normal conditions, death directly causes the dendrite degeneration observed in ddaA, ddaF and ddaB at 3-6 h APF. Similar observations made after killing da neurons by laser ablation support this proposition (Williams and Shepherd, 2002).

Pruning of da neurons by local degeneration and branch retraction

Local degeneration

Pruning of the dendrites of ddaD and ddaE starts between 6 and 10 h APF and is largely complete by 24 h APF (Fig. 1). Our time-lapse movies reveal that dendrites undergo deconstruction by two different cellular mechanisms: local degeneration (Watts et al., 2003) and branch retraction.

During local degeneration, branches are detached from the main arbor and undergo fragmentation (Fig. 3A,E). Watts et al. (Watts et al., 2003) found that axons and dendrites of mushroom body γ neurons undergo local degeneration: between 4 and 6 h APF the processes undergo blebbing, and by 8 h APF most of the dendritic arbor has been removed. By 18 h APF the axons have fragmented, and during that time there was no evidence to suggest that γ neurons undergo retraction. Similarly, larval projection neurons in the olfactory lobe undergo local degeneration (Marin et al., 2005).

A key step in local degeneration appears to be severing, which we were able to visualize with time-lapse movies. Severing happens in one of two ways, depending on position within the arbor. In proximal regions severing is preceded by thinning (Fig. 3B). Once a branch has thinned, it severs and the stump retracts, while the separated arbor undergoes fragmentation. We found that beads adjacent to thinning regions contain abundant Futsch and tub::GFP, whereas these are lacking in the thinned regions, suggesting that the bulk of the microtubule cytoskeleton is lost in these focal regions. This supports observations by Watts et al. (Watts et al., 2003) that myc-marked tubulin disappears from pruning γ neurons before the axon is lost. Similarly, Bishop et al. (Bishop et al., 2004) showed that just prior to shedding 'axosomes', the proximal region of a retracting axon becomes devoid of organized microtubules. When neurons express EcR^{DN}, the caliber of the proximal branches does not change, suggesting that a redistribution of the microtubule cytoskeleton fails and proximal severing is subsequently blocked.

The second type of severing occurs at more distal sites within the arbor (Fig. 3C). Here there is no thinning and only occasional beading; thus it is possible that different mechanisms are responsible for severing at distal sites. Nevertheless, distal severing is also suppressed in neurons that express EcR^{DN}, suggesting that a destabilization is also important here.

After severing, both proximal and distally detached branches undergo fragmentation. The branches thin whilst beads form along their length (Fig. 3D) and break at multiple sites, generating GFP blebs that are removed by phagocytes (see below). Although most of the events observed in branch fragmentation during pruning appear similar to those seen in the arbors of dying da neurons, an exception is the appearance of filopodia. When we have simultaneously imaged the microtubule cytoskeleton and the membrane in pruning neurons, we often find filopodia are coincident with the areas of microtubule disorganization (Fig. 4C). Bray et al. (Bray et al., 1978) found lateral filopodia when they applied colcemid to chick neurons in culture. Filopodia do not appear on the arbors of the doomed cells as the cells are undergoing programmed cell death. However, when cell death is blocked by expression of p35 these cells later show abundant filopodia as their dendrites are removed (Fig. 2E). This suggests a fundamental difference between the dendrite removal observed during the pruning of ddaD and ddaE, and that seen in cells that undergo programmed cell death.

Branch retraction

The primary branches of ddaD and ddaE can be retracted as shown in Fig. 3E. These retraction events occurred in 6/17 neurons imaged and the branches of such neurons often possessed many filopodia. When retraction events happen, local degeneration may still occur in secondary branches and on other primary branches nearby. It is somewhat problematic to apportion what percentage of pruning is due to retraction and what is due to severing and fragmentation, as they both appear to happen simultaneously, e.g. where a branch is in the process of distal retraction and suddenly is severed at a more proximal site.

The dendrites of neurons expressing EcR^{DN} form bulb-like structures on their distal tips and produce few if any filopodia. Local degeneration is blocked in these neurons, but they do eventually remove their dendrites by retraction. A number of scenarios could explain this retraction phenotype. It is possible that EcR^{DN} does not block all ecdysone signaling and so the

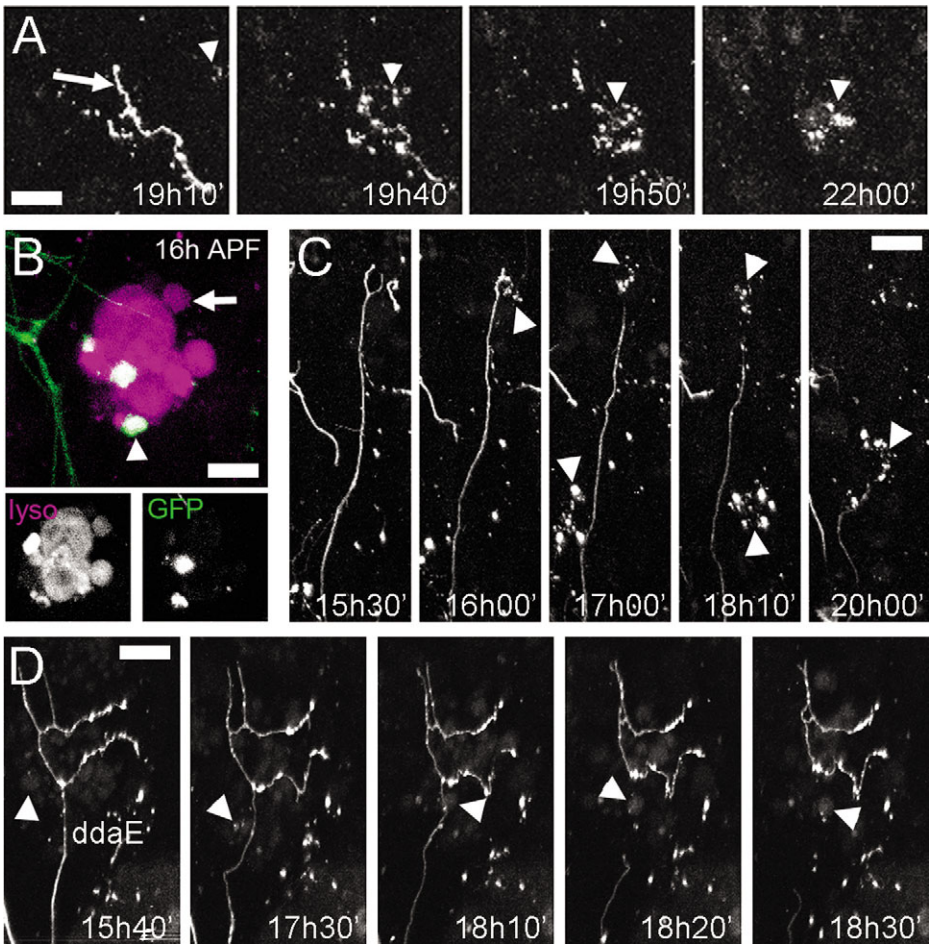

Fig. 7. Phagocytic blood cells engulf neuronal debris and attack intact dendrites during pruning. (A) Frames from a time-lapse movie of da neurons (*C161-GAL4>CD8::GFP*) showing phagocytic blood cell consuming a detached dendrite branch. At 19 h 10 min a weakly labeled phagocyte enters from the right (arrowhead). By 19 h 40 min the phagocyte has moved close to the severed branch. At 19 h 50 min the branch fragments and by 20 h 50 min the phagocyte, is strongly labeled with GFP. Scale bar: 20 μm. (B) A projected z-stack of a phagocyte labeled with LysoTracker DND-99 in a wild-type animal (*C161-GAL4>CD8::GFP*) showing details of vesicles. Different sized vesicular compartments that do not contain GFP are evident (arrow) along with ones that do (arrowhead). Scale bar: 7 μm. (C) Phagocyte attacking distal tip of ddaE. Selected frames from a time-lapse movie. At 16 h 00 min a phagocyte can be seen on the right which then comes into contact with the distal tip of the branch (top arrowhead). By 17 h 00 min the branch and the phagocyte are no longer in contact and the phagocyte contains more GFP than before. Another phagocyte crosses the branch from the lower left (arrowhead) attacking the retracting end of the primary branch between 19 h 10 min and 20 h 30 min. Scale bar: 35 μm. (D) Phagocytic blood cells attack intact proximal branches. At 15 h 40 min a phagocyte enters the field from the left. Between 15 h 40 min and 17 h 30 min it moves close to the pruning arbor of ddaE (arrowhead). Between 18 h 10 min and 18 h 20 min the branch is severed at the site where the phagocyte is located. A small bleb of GFP, derived from the severed branch is internalized by the phagocyte and moves away with the blood cell (18 h 30 min arrowhead). Scale bar: 25 μm.

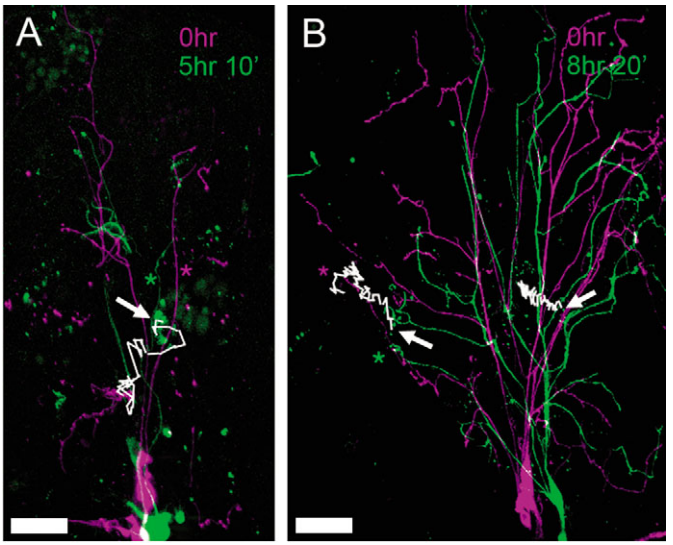

Fig. 8. Phagocyte behavior changes when pruning is blocked. False color indicates the different frames of the respective time-lapse movies; magenta, the first frame and green the final frame. The path of a phagocyte through all of the frames is recorded as a white line, and the final destination denoted with an arrow. (A) In a movie of a wild-type animal (*C161-GAL4>CD8::GFP*) starting at 0 h (~14 h APF) the phagocyte tracks around the ventral branch of ddaD until it is severed and then moves to the right attacking the retracting branch of ddaE. (B) In a movie of EcR^{DN} expressing neurons (*C161-GAL4>EcR^{DN};CD8::GFP*) starting at 0 h (14 h 20 min APF) two phagocytes have been tracked. The phagocyte to the left follows the distal tip of the branch, removing pieces as it retracts. The other phagocyte is found near the proximal arbor and moves slowly across the field and does not interact with the 'non-thinned' branches. Scale bar: 30 μm.

cell intrinsic ecdysone pruning program has not been entirely eliminated. It is also possible, but unlikely, that the EcR^{DN} results in a non-specific 'neomorphic' as the specificity of this reagent has been demonstrated by Cherbas et al. (Cherbas et al., 2003). The other possibility is that EcR^{DN} completely blocks ecdysone signaling and that another parallel intrinsic signaling pathway plays a role in dendrite retraction. It is most likely that EcR^{DN} completely blocks ecdysone signaling and that the phenotype we see reveals extrinsic factors that are important for dendrite pruning under wild-type conditions. The neuron-specific expression of EcR^{DN} means that ecdysone signaling is only disrupted in the neuron and that the local environment can undergo its normal hormone induced changes.

Remodeling of the dendritic target

A dorsal region of the epidermis is the target for the dendrites of ddaD and ddaE. Two potential interactions could be taking place between the target and pruning arbor. The epidermis could be sending an instructive signal causing the arbor to prune or there could be a passive loss of epidermal contacts as the larval epidermis is replaced. To explore the latter possibility we made movies at the time when ddaD and ddaE are pruning. It has been widely held that the larval epidermal cells are only removed by the migrating front of adult epidermal cells derived from the histoblast nest (Madhavan and Madhavan, 1980; Fristrom and Fristrom, 1993). To our surprise we found that during early metamorphosis larval cells are removed at sites distant from the histoblast migration front (Fig. 6B). The epidermal cells are removed by phagocytic blood cells and the cells that are removed do not show obvious signs of apoptosis before being contacted by the phagocyte. This suggests that the larval cells are killed by a phagocytosis-induced cell death as described in *C. elegans* (Reddien et al., 2001) and *Drosophila* (Mergliano and Minden, 2003). Importantly, when a larval cell is removed, other cells move to compensate for its loss. Thus the epidermis becomes a dynamic substrate during prepupal and early pupal development and this movement may result in shearing events in distal dendritic branches and could explain the phenomenon of distal severing without thinning. Likewise, the disruption of neuron-epidermal contacts may contribute to the retraction of primary branches seen in an extreme form when neurons express the EcR^{DN}.

Phagocytes scavenge neuronal debris and attack intact branches

In flies with GFP-expressing neurons we found that phagocytic blood cells also became labeled, which in turn allowed us to visualize their behavior in early pupae. Our time-lapse movies reveal that phagocytes are intimately involved in the fragmentation and engulfment of severed dendritic branches. The sequence in Fig. 7A shows a faintly labeled phagocyte coming into close proximity with a severed and beaded branch. After contact the branch fragments and the phagocyte consumes the debris, thereby becoming strongly labeled with GFP. The degenerating branches of dying da neurons share the same fate, as we see GFP blebs move off in random directions following fragmentation because of their movement in phagocytes. In the vertebrate nervous system, cells with phagocytic capacity play a scavenger role, clearing up the cellular debris that results from Wallerian degeneration and normal developmental cell death (Hirata and Kawabuchi, 2002; Mallat et al., 2005).

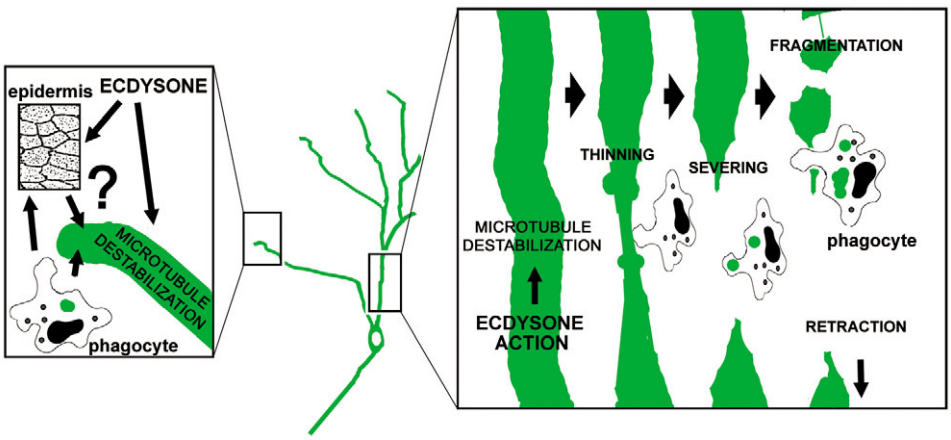

Fig. 9. Summary of cellular mechanisms of da neuron dendrite pruning.

During early metamorphosis, glial processes infiltrate the mushroom body neuropil when axons are undergoing local degeneration (Awasaki and Ito, 2004; Watts et al., 2004). Ultrastructure studies show that remnants of labeled neurons appear in these glia (Watts et al., 2004). Awasaki and Ito (Awasaki and Ito, 2004) also suggest that glia play an active role in the destruction of the axons, since inhibiting endocytosis in the glia stopped infiltration and blocked axon pruning. Our time-lapse data also reveal that in the periphery phagocytic blood cells also attack intact dendritic branches. As shown in Fig. 7B,C, phagocytes both attack the distal tips of retracting branches and sever branches at proximal positions. We do not observe the phenomenon of proximal severing by phagocytes in every movie, which suggests that either severing can result from other forces such as the shearing action of the reorganizing epidermis, or we are not seeing all the phagocyte/neuron interactions because only a fraction of phagocytes are labeled. Nevertheless our data shows that phagocytic cells have an active role in the pruning of peripheral neurons.

During the clearance of apoptotic cells, phagocytes are known to recognize specific 'eat me' signals on the surface of a dying cell (Savill and Fadok, 2000). Are the phagocytes recognizing similar 'bite me' signals on the arbors of the pruning da neurons? Our observations suggest that they are targeting specific regions of branches that show signs of destabilization. Targeting of destabilized regions is especially obvious from the behavior of phagocytes encountering neurons expressing EcR^{DN}. These phagocytes ignore the stable proximal regions of the arbor and instead only attack the distal tips (Fig. 8).

Taken together, our data show that the pruning of the da neuron dendrites during metamorphosis is achieved by local degeneration and branch retraction. We propose that these phenomena are controlled by both intrinsic and extrinsic cellular mechanisms (Fig. 9). The initiation of pruning by the steroid hormone ecdysone results in the destabilization of the microtubule cytoskeleton within the dendritic arbor. This loss of microtubules results in the severing of the branches, either by attacking phagocytes or possibly from shearing forces produced in the remodeling epidermis. Severed dendritic branches undergo a distinctive 'beading', similar to redistribution of the microtubule cytoskeleton found in the arbors of dying cells. Phagocytes are intimately involved in the fragmentation and consumption of severed branches, which leads to a rapid clearance of cellular debris.

We expect that the mechanisms described here are not restricted to the dendrites of *Drosophila* sensory neurons undergoing remodeling during metamorphosis. It will be very interesting to learn which mechanisms used by developing cells to remove their neuritic processes are employed by cells following trauma or the onset of disease.

We would like to thank Wayne Johnson, Lucy Cherbas, Allan Spradling and the Bloomington for fly stocks, the DSHB for monoclonal antibodies, Sara Lennox for technical assistance, Margrit Schubiger, Janet Altman and Lisa Marin for reading the manuscript and Sanjay Sane for helpful discussions. Research was supported by NIH grant NS13079.

Supplementary material

Supplementary material for this article is available at
http://dev.biologists.org/cgi/content/full/132/16/3631/DC1

References

Ainsley, J. A., Pettus, J. M., Bosenko, D., Gerstein, C. E., Zinkevich, N., Anderson, M. G., Adams, C. M., Welsh, M. J. and Johnson, W. A. (2003). Enhanced locomotion caused by loss of the *Drosophila* DEG/ENaC protein Pickpocket1. *Curr. Biol.* **13**, 1557-1563.

Awasaki, T. and Ito, K. (2004). Engulfing action of glial cells is required for programmed axon pruning during *Drosophila* metamorphosis. *Curr. Biol.* **14**, 668-677.

Bagri, A., Cheng, H. J., Yaron, A., Pleasure, S. J. and Tessier-Lavigne, M. (2003). Stereotyped pruning of long hippocampal axon branches triggered by retraction inducers of the semaphorin family. *Cell* **113**, 285-299.

Beirowski, B., Adalbert, R., Wagner, D., Grumme, D. S., Addicks, K., Ribchester, R. R. and Coleman, M. P. (2005). The progressive nature of Wallerian degeneration in wild-type and slow Wallerian degeneration (WldS) nerves. *BMC Neurosci.* **6**, 6.

Bishop, D. L., Misgeld, T., Walsh, M. K., Gan, W. B. and Lichtman, J. W. (2004). Axon branch removal at developing synapses by axosome shedding. *Neuron* **44**, 651-661.

Burek, M. J. and Oppenheim, R. W. (1996). Programmed cell death in the developing nervous system. *Brain Pathol.* **6**, 427-446.

Bray, D., Thomas, C. and Shaw, G. (1978). Growth cone formation in cultures of sensory neurons. *Proc. Natl. Acad. Sci. USA* **75**, 5226-5229.

Cherbas, L., Hu, X., Zhimulev, I., Belyaeva, E. and Cherbas, P. (2003). EcR isoforms in *Drosophila*: testing tissue-specific requirements by targeted blockade and rescue. *Development* **130**, 271-284.

Clarkson, M. and Saint, R. (1999). A His2AvDGFP fusion gene complements a lethal His2AvD mutant allele and provides an in vivo marker for *Drosophila* chromosome behavior. *DNA Cell Biol.* **18**, 457-462.

Cowan, W. M., Fawcett, J. W., O'Leary, D. D. and Stanfield, B. B. (1984). Regressive events in neurogenesis. *Science* **225**, 1258-1265.

Fristrom, D. and Fristrom, J. W. (1993). The metamorphic development of the adult epidermis. In *The Development of Drosophila melanogaster*. Vol II (ed. M. Bate and A. Martinez), pp. 843-897. Cold Spring Harbor, NY: Cold Spring Harbor Laboratory.

Grieder, N. C., de Cuevas, M., Spradling, A. C. (2000). The fusome organizes the microtubule network during oocyte differentiation in *Drosophila*. *Development* **127**, 4253-4264.

Grueber, W. B., Jan, L. Y. and Jan, Y. N. (2002). Tiling of the *Drosophila* epidermis by multidendritic sensory neurons. *Development* **129**, 2867-2878.

Grueber, W. B., Jan, L. Y. and Jan, Y. N. (2003). Different levels of the homeodomain protein cut regulate distinct dendrite branching patterns of *Drosophila* multidendritic neurons. *Cell* **112**, 805-818.

Hartenstein, V. and Posakony, J. W. (1989). Development of adult sensilla on the wing and notum of *Drosophila melanogaste*r. *Development* **107**, 389-405.

He, Y., Yu, W., Baas, P. W. (2002). Microtubule reconfiguration during axonal retraction induced by nitric oxide. *J. Neurosci.* **22**, 5982-5991.

Hirata, K. and Kawabuchi, M. (2002). Myelin phagocytosis by macrophages and nonmacrophages during Wallerian degeneration. *Microsc. Res. Tech.* **57**, 541-547.

Hummel, T., Krukkert, K., Roos, J., Davis, G. and Klambt, C. (2000). *Drosophila* Futsch/22C10 is a MAP1B-like protein required for dendritic and axonal development. *Neuron* **26**, 357-370.

Keller-Peck, C. R., Walsh, M. K., Gan, W. B., Feng, G., Sanes, J. R. and Lichtman, J. W. (2001). Asynchronous synapse elimination in neonatal motor units: studies using GFP transgenic mice. *Neuron* **31**, 381-394.

Lee, T. and Luo, L. (1999). Mosaic analysis with a repressible cell marker for studies of gene function in neuronal morphogenesis. *Neuron* **22**, 451-461.

Lee, T., Marticke, S., Sung, C., Robinow, S. and Luo, L. (2000). Cell-autonomous requirement of the USP/EcR-B ecdysone receptor for mushroom body neuronal remodeling in *Drosophila*. *Neuron* **28**, 807-818.

Levine, R. B. and Weeks, J. C. (1996). Cell culture approaches to understanding the actions of steroid hormones on the insect nervous system. *Dev. Neurosci.* **18**, 73-86.

Luo, L. and O'Leary, D. M. (2005). Axon retraction and degeneration in development and disease. *Annu. Rev. Neurosci.* **28**, 127-156.

Madhavan, M. M. and Madhavan, K. (1980). Morphogenesis of the epidermis of adult abdomen of *Drosophila*. *J. Embryol. Exp. Morphol.* **60**, 1-31.

Mallat, M., Marin-Teva, J. L. and Cheret, C. (2005). Phagocytosis in the developing CNS: more than clearing the corpses. *Curr. Opin. Neurobiol.* **15**, 101-107.

Marin, E. C., Watts, R. J., Tanaka, N. K., Ito, K. and Luo, L. (2005).

Developmentally programmed remodeling of the *Drosophila* olfactory circuit. *Development* **132**, 725-737.

Mergliano, J. and Minden, J. S. (2003). Caspase-independent cell engulfment mirrors cell death pattern in *Drosophila* embryos. *Development* **130**, 5779-5789.

Nakamura, H. and O'Leary, D. D. (1989). Inaccuracies in initial growth and arborization of chick retinotectal axons followed by course corrections and axon remodeling to develop topographic order. *J. Neurosci*. **9**, 3776-3795.

O'Leary, D. D. and Koester, S. E. (1993). Development of projection neuron types, axon pathways, and patterned connections of the mammalian cortex. *Neuron* **10**, 991-1006.

Perry, V. H., Henderson, Z. and Linden, R. (1983). Postnatal changes in retinal ganglion cell and optic axon populations in the pigmented rat. *J. Comp. Neurol*. **219**, 356-368.

Reddien, P. W., Cameron, S. and Horvitz, H. R. (2001). Phagocytosis promotes programmed cell death in *C. elegans*. *Nature* **412**, 198-202.

Reyes, R., Haendel, M., Grant, D., Melancon, E. and Eisen, J. S. (2004). Slow degeneration of zebrafish Rohon-Beard neurons during programmed cell death. *Dev. Dyn*. **229**, 30-41.

Savill, J. and Fadok, V. (2000). Corpse clearance defines the meaning of cell death. *Nature* **407**, 784-788.

Schubiger, M., Wade, A. A., Carney, G. E., Truman, J. W. and Bender, M. (1998). *Drosophila* EcR-B ecdysone receptor isoforms are required for larval molting and for neuron remodeling during metamorphosis. *Development* **125**, 2053-2062.

Schubiger, M., Tomita, S., Sung, C., Robinow, S. and Truman, J. W. (2003). Isoform specific control of gene activity in vivo by the *Drosophila* ecdysone receptor. *Mech. Dev.* **120**, 909-918.

Sievers, C., Platt, N., Perry, V. H., Coleman, M. P. and Conforti, L. (2003). Neurites undergoing Wallerian degeneration show an apoptotic-like process with Annexin V positive staining and loss of mitochondrial membrane potential. *Neurosci. Res.* **46**, 161-169.

Smith, S. A. and Shepherd, D. (1996). Central afferent projections of proprioceptive sensory neurons in *Drosophila* revealed with the enhancer-trap technique. *J. Comp. Neurol.* **364**, 311-323.

Taylor, B. J. (1989). Sexually dimorphic neurons in the terminalia of *Drosophila melanogaster*: I. Development of sensory neurons in the genital disc during metamorphosis. *J. Neurogenet.* **5**, 173-192.

Truman, J. W. (1996). Steroid receptors and nervous system metamorphosis in insects. *Dev. Neurosci*. **18**, 87-101.

Truman, J. W., Schuppe, H., Shepherd, D., Williams, D. W. (2004). Developmental architecture of adult-specific lineages in the ventral CNS of *Drosophila*. *Development* **131**, 5167-5184.

Usui-Ishihara, A., Simpson, P. and Usui, K. (2000). Larval multidendrite neurons survive metamorphosis and participate in the formation of imaginal sensory axonal pathways in the notum of Drosophila. *Dev. Biol*. **225**, 357-369.

Waller, A. (1850). Experiments on the section of the glossopharyngeal and hypoglossal nerves of the frog, and observations of the alterations produced thereby in the structure of primitive fibres. *Philos. Trans. R. Soc. London Ser. B* **140**, 423-429.

Watts, R. J., Hoopfer, E. D. and Luo, L. (2003). Axon pruning during *Drosophila* metamorphosis: evidence for local degeneration and requirement of the ubiquitin-proteasome system. *Neuron* **38**, 871-885.

Watts, R. J., Schuldiner, O., Perrino, J., Larsen, C. and Luo, L. (2004). Glia engulf degenerating axons during developmental axon pruning. *Curr. Biol.* **14**, 678-684.

Williams, D. W. and Shepherd, D. (1999). Persistent larval sensory neurons in adult *Drosophila melanogaster*. *J. Neurobiol*. **39**, 275-286.

Williams, D. W. and Shepherd, D. (2002). Persistent larval sensory neurones are required for the normal development of the adult sensory afferent projections in *Drosophila*. *Development* **129**, 617-624.

Williams, D. W. and Truman, J. W. (2004). Mechanisms of dendritic elaboration of sensory neurons in *Drosophila*: insights from in vivo time lapse. *J. Neurosci*. **24**, 1541-1550.

Zhai, Q., Wang, J., Kim, A., Liu, Q., Watts, R., Hoopfer, E., Mitchison, T., Luo, L. and He, Z. (2003). Involvement of the ubiquitin-proteasome system in the early stages of wallerian degeneration. *Neuron* **39**, 217-225.

Zheng, X., Wang, J., Haerry, T. E., Wu, A. Y., Martin, J., O'Connor, M. B., Lee, C. H. and Lee, T. (2003). TGF-beta signaling activates steroid hormone receptor expression during neuronal remodeling in the *Drosophila* brain. *Cell* **112**, 303-315.